HOKKAIDO UNIVERSITY

Title	In situ FTIR study on the formation and adsorption of CO on alumina-supported noble metal catalysts from H2 and CO2 in the presence of water vapor at high pressures
Author(s)	Yoshida, Hiroshi; Narisawa, Satomi; Fujita, Shin-ichiro et al.
Citation	Physical Chemistry Chemical Physics, 14(14), 4724-4733 https://doi.org/10.1039/c2cp23590k
Issue Date	2012-04-14
Doc URL	https://hdl.handle.net/2115/51998
Rights	Phys. Chem. Chem. Phys., 2012,14, 4724-4733 - Reproduced by permission of the PCCP Owner Societies
Type	journal article
File Information	PCCP14-14_4724-4733.pdf

Hokkaido University Collection of Scholarly and Academic Papers : HUSCAP

In situ FTIR study on the formation and adsorption of CO on alumina-supported noble metal catalysts from H_2 and CO_2 in the presence of water vapor at high pressures

Hiroshi Yoshida, Satomi Narisawa, Shin-ichiro Fujita, Liu Ruixia, and Masahiko Arai*

Division of Chemical Process Engineering, Faculty of Engineering,
Hokkaido University, Sapporo 060-8628, Japan
* Corresponding author. E-mail: marai@eng.hokudai.ac.jp

(Abstract)
The formation and adsorption of CO from CO_2 and H_2 at high pressures were studied over alumina-supported noble metal catalysts (Pt, Pd, Rh, Ru) by *in situ* FTIR measurements. To examine the effects of surface structure of supported metal particles and water vapor on the CO adsorption, FTIR spectra were collected at 323 K with untreated and heat (673 K) treated catalysts in the absence and presence of water (H_2O, D_2O). It was observed that the adsorption of CO occurred on all the metal catalysts at high pressures, some CO species still remained adsorbed under ambient conditions after the high pressure FTIR measurements, and the frequencies of the adsorbed CO species were lower either for the heat treated samples or in the presence of water vapor. It is assumed that the CO absorption bands on atomically smoother surfaces appear at lower frequencies and that water molecules are adsorbed more preferentially on atomically rough surfaces rather than CO species.

1. Introduction

Dense phase CO_2 is one of interesting components for homogeneous and heterogeneous (multiphase) reaction media.[1-8] When hydrogenation reactions are conducted with supported metal catalysts in the presence of pressurized H_2 and CO_2, there is a possibility of the formation and adsorption of CO through reverse water gas shift reaction or other pathways. Using *in situ* high pressure FTIR techniques, a few authors investigated this phenomenon important in catalytic hydrogenation and other reactions in the presence of dense phase CO_2 .[9-15] Baiker *et al.* used attenuated total reflection infrared spectroscopy (ATR-IR) to follow the reaction of CO_2 with H_2 over alumina-supported Pt catalyst in the form of thin film in cyclohexane at 313 K.[9,10,12] It is indicated that carbonate-like species are formed from CO_2 adsorbed on the support and then react with H_2, forming CO. The formation of CO was responsible for the catalyst deactivation observed in hydrogenation of ethyl pyruvate in supercritical CO_2. Subramaniam *et al.* investigated the formation and adsorption of CO over hydrogenation catalysts (alumina-supported Pd, Ru, Ni) at 13.6 MPa and at 342 K using *in situ* Fourier transform infrared spectroscopy (FTIR) technique using pelletized catalyst samples.[13] They state that CO is formed through the reverse water gas shift reaction ($CO_2 + H_2 \rightarrow CO + H_2O$) on Pd but not on Ru and Ni; so, the latter two metal catalysts may be suitable for hydrogenation in the presence of dense phase CO_2 because catalyst deactivation due to CO adsorption would be unlikely to occur. The present authors made a similar *in situ* FTIR study with alumina- and carbon-supported Rh catalysts at 323 K and at different CO_2 pressures.[15] The formation and adsorption of CO was observed on both catalysts. The CO species adsorbed on the carbon-supported catalyst disappeared when the pressure was released to ambient pressure, while some CO species still remained on the alumina-supported catalyst. That is, CO is strongly adsorbed on the surface of alumina-supported Rh particles and this may explain its rapid deactivation during hydrogenation of phenol in the mixture of H_2 (4 MPa) + CO_2 (8 MPa or 14 MPa).

Those results demonstrate the significance of CO formed from $H_2 + CO_2$ for heterogeneous catalytic hydrogenation and other reactions, including those in CO_2-dissolved expanded liquid phases. There still remains one important issue, which is the role of water formed along with CO from $H_2 + CO_2$ in the formation and adsorption of CO and in the catalytic reactions. Lefferts *et al.* investigated CO adsorption and oxidation over alumina-supported Pt and Pd catalysts in gas and aqueous phases by ATR-IR technique.[16,17] From the observations of red-shift and intensity enhancement of

CO absorption band, they assume that water may modify the potential of supported metal particles and interact directly with CO molecules on their surfaces in aqueous phase. It is also assumed that the oxidation of CO is promoted by the formation of an activated complex of CO and water molecules. For the CO adsorption on a Ru(001) single crystal, Nakamura and Ito observed a similar red-shift of linear CO absorption band in the presence of water and the red-shift was ascribed to an electron transfer from a lone pair of a water molecule to CO $2\pi^*$,[18] in common for the surfaces of Ru(001) under both vacuum and solution conditions. Using ATR-FTIR, a similar red-shift was also reported by Layman *et al.* for a hydrated Ru/Al_2O_3 catalyst, which was explained by dipole-dipole interaction between co-adsorbed CO and water molecules.[19] In contrast, Solymosi *et al.* did not observe such a significant shift for a Ru/Al_2O_3 catalyst that was exposed to CO (ca. 67 Pa) in the presence of water (ca. 13 Pa) at 300 K.[20] Note that there is only a small amount of water present in the reaction systems of our interest, which exists in CO_2-rich gas phase, CO_2-dissolved organic liquid phase, or at interface between gas and organic liquid phases. Recently, the authors have communicated that the selective hydrogenation of aromatic nitro compounds into the corresponding amines is achieved in the presence of pressurized CO_2 and, in addition, the positive effect of CO_2 pressurization can appear at a lower pressure (around 1 MPa) in the presence of water.[21] But, the influence of water addition is still not clear at present.

Based on those previous interesting observations in multiphase mixtures including CO_2, H_2, and water, the present work was undertaken to investigate the formation and adsorption of CO from the mixture of CO_2 and H_2 on several alumina-supported noble metal (Pt, Pd, Rh, Ru) catalysts in the presence of water vapor at high pressures. *In situ* FTIR technique was used to examine the state of CO adsorbed on the catalysts at different pressures, in which either CO_2 + H_2 or CO was a source of CO and either H_2O or D_2O was used. The influence of water vapor on the CO formation and adsorption was discussed in detail. It is proposed that CO molecules formed from the CO_2 and H_2 mixture are adsorbed on different surface sites and those on high Miller index surfaces (atomically rough surfaces) are replaced by water molecules.

2. Experimental

2.1. Catalyst samples

Four Al_2O_3-supported Pt, Pd, Rh, and Ru catalysts were purchased from Wako. The catalyst samples were used without further treatment and with reduction by flowing H_2

(99.99 % in volume) at 673 K for 3 h in a furnace, which will be referred to as untreated (UT) and heat treated (HT) samples, respectively, in the following. These Al_2O_3-supported metal catalysts were examined by transmission electron microscopy (JEOL JEM-2000ES). The catalyst was ground in a mortar and dispersed in ethanol; a few drops of the suspension were put on a carbon-coated collodion film on TEM grid and dried under ambient conditions. The metal particle size distributions were determined on the TEM pictures obtained. Those results will be presented in 3.1.

2.2. *In situ* FTIR measurements

An Al_2O_3-supported metal catalyst (30 mg) was ground in a mortar and the catalyst powder was pressurized at 50 MPa for 1 h to prepare a catalyst pellet. The pelletized catalyst sample was placed in a high-pressure FTIR cell (JASCO). The cell volume was 1.5 cm^3 and the optical pathway was 1 cm. The cell was purged by H_2 gas (99.99 %) a few times to remove the air and heated to 343 K; H_2 was further introduced to 4 MPa and maintained at this temperature for 1 h. The cell was cooled to 323 K, purged again by atmospheric H_2 a few times, and introduced with high pressure H_2 and then CO_2 (99.99%). *In situ* FTIR measurements were made at a H_2 pressure of 4 MPa and at different CO_2 pressures up to 20 MPa using a JASCO FTIR-620 spectrometer with a resolution of 2 cm^{-1}. The spectra collected in the presence of 4 MPa H_2 and CO_2 at different pressures were used as background. After the measurements at high pressures, the gases in the cell were released to ambient pressure and FTIR spectra were further collected. The FTIR setup and procedures used were described in more detail in previous works.[15,22,23] Moreover, similar FTIR measurements were made in the presence of water vapor, in which 10 μL of water was put into the bottom of the cell loaded with the pelletized catalyst and then the sample was treated by H_2 in the same manners as described above. *In situ* FTIR spectra were collected at 4 MPa H_2, at 20 MPa CO_2, and at 323 K using the spectrum measured in the presence of the H_2 gas and water as background. The vapor pressure of water is 12.3 kPa at this temperature.[24]

The adsorption of CO was also measured in similar procedures using CO instead of CO_2 + H_2 for a selected sample. The pelletized catalyst sample reduced with H_2, the FTIR cell was purged by H_2 a few times, the sample was exposed to 1% CO (He balance) and the FTIR spectra were collected in the presence of water vapor. The FTIR measurement was also made in the absence of water; then, a small amount of water was added into the cell and the FTIR spectra were further measured. The water was introduced into the cell with a syringe through a small hole where nitrogen gas was flowing out.

3. Results and discussion

3.1. TEM of Al_2O_3-supported Noble Metal Catalysts

Al_2O_3-supported Pt, Pd, Rh, and Ru catalysts were used in the present FTIR experiments. The FTIR measurements were made for the pelletized catalysts with no pretreatment (UT-samples) and treatment by H_2 at 673 K for 3 h (HT-samples). Figure 1 and Figure 2 display TEM pictures of those UT and HT catalyst samples and metal particle size distributions determined on them, respectively. The heat treatment caused the particle growth for the four metal catalysts. The surface of supported noble metal particles in UT- and HT-samples was examined by X-ray photoelectron spectroscopy using a selected couple of UT- and HT-Rh/Al_2O_3 catalysts. Although these samples were different in the size of metal particles (Figures 1 & 2), no significant difference was observed in the XPS spectra (as given in Supporting Information).

Figure 1, Figure 2

In the following, *in situ* FTIR spectra measured with those different supported noble metal catalysts at high pressures will be presented.

3.2. Formation and Adsorption of CO from CO_2 + H_2 in the Absence of Water

In situ high-pressure FTIR spectra were collected with the four Al_2O_3 supported noble metal catalysts, untreated (UT) and heat-treated (HT), under different conditions. A few different types of CO adsorption were detected and their structures were determined according to the literature, as summarized in Table 1.

Table 1

(a) Pt/Al_2O_3 Figures 3A gives FTIR spectra of UT-Pt/Al_2O_3 collected on exposure to H_2 + CO_2 at 323 K and at different pressures. The CO absorption band is seen after the pre-reduction with 4 MPa H_2 at 343 K in the absence of CO_2 (Figure 3A, line 1). Figure 4 shows the FTIR spectra of the same sample in a wider frequency range, including the result after the reduction with H_2 at 0.1 MPa as well. It is indicated that the CO absorption band appears even after the reduction with H_2 at a lower pressure of 0.1 MPa, similar to that at 4 MPa. Figure 4 shows that there is an absorption band at

1650 cm^{-1} before the reduction, which may be assigned to carbonate type species [47] and physisorbed water on the support. The amount of such carbonate species should be small and so the other expected weaker absorption band at about 1250 cm^{-1} is not clear. This band at 1650 cm^{-1} decreases in the intensity after the reduction but new absorption bands appear at 1750 cm^{-1} and 2050 cm^{-1} assignable to the CO species. It is assumed, therefore, that the CO species seen after the pre-treatment with H_2 result from the reduction of the surface carbonate species on the catalyst sample. This is the same for the other samples of Rh/Al_2O_3 and Ru/Al_2O_3 catalysts except for Pd/Al_2O_3. The CO_2-derived species should exist on the surface of Al_2O_3 but not on the metals since the same adsorbed species were seen for metal-free Al_2O_3 support itself (the corresponding FTIR spectra are given in Supporting Information).

Figure 3A shows that the absorption bands exist at 1750 – 1850 cm^{-1} and 1900 – 2100 cm^{-1}, which may be ascribed to bridge type and linear type of CO adsorbed on the surface of supported Pt particles, respectively.[25-32] When the CO_2 pressure is raised, the CO absorption band at 1900 – 2100 cm^{-1} increases while that at 1700 – 1850 cm^{-1} does not change so much. Namely, the amount of linearly adsorbed CO species increases with the pressure up to about 10 MPa and remains almost unchanged at higher pressures. When the pressure was released to ambient pressure after the high-pressure measurements, some CO species were still present on the catalyst.

Figure 3, Figure 4

Similar results were obtained with HT-Pt/Al_2O_3 sample (Figure 3B). As mentioned above, the absorption band at 1900 – 2100 cm^{-1}, which has a peak at about 2080 cm^{-1} and a shoulder peak at about 2040 cm^{-1}, changes in intensity with CO_2 pressure. The intensity of the main peak at 2080 cm^{-1} against the shoulder peak at 2020 cm^{-1} seems to be larger for the HT sample having a larger metal particle size of 4.3 nm compared to that for the above-mentioned UT sample of 3.4 nm. The absorption band located at 2080 cm^{-1} is assigned to CO adsorbed on Pt terrace sites, while that at 2040 cm^{-1} is ascribable to CO adsorbed on edge, corner and/or kink Pt sites.[26, 29-32] The fraction of the terrace sites would be larger for the surface of larger Pt particles, which may explain the relatively stronger intensity of the main peak at the higher frequency as observed for the HT-Pt/Al_2O_3. Previously, Xu and Yates investigated the adsorption of CO on Pt(335) and Pt(112) surfaces.[26] They indicated that the frequency of linear CO on the Pt(335) step site was 2070 cm^{-1} but 2064 cm^{-1} on the Pt(112) step site, due to the difference in the step density, for which the surface of Pt(335) was more similar to that

of larger Pt particles rather than Pt(112).

(b) Pd/Al_2O_3 *In situ* FTIR results obtained with UT-Pd/Al_2O_3 are given in Figure 5A. Two CO absorption bands may be distinguished at 1980 – 2080 cm^{-1} and 1760 – 1980 cm^{-1}. Although the presence of carbonate species was detected on the catalyst (not shown), no CO adsorption was observed after the reduction (before the introduction of CO_2). The former is assigned to CO species linearly adsorbed on Pd while the latter to the adsorbed CO species of bridge type.[33-36] The absorption band of the bridge CO is larger than that of linear CO and increases with CO_2 pressure. It is reported that the extinction coefficient is larger for the bridge CO species on Pd than for the linear ones.[48] Similar to Pt/Al_2O_3, the CO species adsorbed on Pd/Al_2O_3 were observed to still remain on the surface when the pressure was lowered to ambient condition.

Figure 5

Figure 5B shows the results with HT-Pd/Al_2O_3 sample and the bridge CO is seen as the main adsorbed species at 1760 – 1980 cm^{-1} for this HT sample as well. The CO absorption bands and their changes with CO_2 pressure are similar to those of the above-mentioned UT sample. The shape of the bridge CO absorption band is not so different between the UT and HT samples, the average particle size being 3.6 nm and 5.5 nm, respectively. So, it is unclear, at present, whether the absorption frequency of these bridge CO species changes with the surface roughness or not from the present results.

(c) Rh/Al_2O_3 Figure 6A gives *in situ* FTIR spectra with UT-Rh/Al_2O_3. Similar to Pt/Al_2O_3, the CO adsorption was detected on Rh under ambient condition after the reduction. It is reported that CO can be adsorbed on Rh in different types of linear, bridged, and twin CO species and the latter one is replaced by hydride CO species in the presence of H_2.[37-40] The absorption band of twin CO appears at a higher frequency (2035 – 2100 cm^{-1}) than that for linear CO (2060 – 2070 cm^{-1}). Then, the absorption band observed at 1900 – 2030 cm^{-1} may be due to the linear CO and/or the hydride CO and that at 1700 – 1900 cm^{-1} to the bridge CO. When the CO_2 pressure was raised, the absorption band of the linear and/or hydride CO species mainly increased. Some CO species remained on depressurization to atmospheric pressure, similar to Pt/Al_2O_3 and Pd/Al_2O_3. In the present work, we detected the formation and adsorption of CO from H_2 + CO_2 mixture at high pressures for Rh/Al_2O_3, similar to Baiker *et al.*

with ATR-IR,[12] but Subramaniam *et al.* did not by transmission FTIR.[13] The latter authors suggest that CO is not formed or may be methanated immediately it is formed.

Figure 6

Similar results were also obtained for HT-Rh/Al_2O_3 sample (Figure 6B). The CO_2 pressurization seems to enhance the CO absorption band at 2035 – 2100 cm^{-1} but not that at 1700 – 1900 cm^{-1}. Comparison of the former bands of the HT- and UT-Rh/Al_2O_3 samples indicates that the shape of the band at 2035 – 2100 cm^{-1} is different and that of the former sample seems to lean to lower frequency. So, the frequency of the linear and/or hydride CO should be higher on smoother surface of larger Rh particles (4.5 nm) in the HT-Rh/Al_2O_3 sample compared to the UT one (3.4 nm).

(d) Ru/Al_2O_3 Alike Pt/Al_2O_3 and Rh/Al_2O_3, the CO adsorption was detected at ambient pressure after the reduction. Figure 7 shows a broad absorption band at 1800 – 2040 cm^{-1}, which may be assigned to linearly adsorbed CO species at about 2020 cm^{-1} and bridge CO species at 1940 cm^{-1}.[41-46] This broad band increases with CO_2 pressure for the UT- and HT-Ru/Al_2O_3 catalysts. Some CO species remained adsorbed on Ru even when the CO_2 pressure was decreased. The shape of the CO absorption band is significantly different between the UT- and HT-Ru/Al_2O_3 samples; the ratio of the higher frequency band against the lower frequency one is larger for the latter sample, which has a larger Ru particle size (3.5 nm) having smoother surfaces, compared to the former UT sample (2.4 nm).

Figure 7

The above-mentioned results with the four Al_2O_3-supported noble metal catalysts are summarized as follows. CO is formed from CO_2 + H_2 mixture at a low temperature of 323 K and at high pressures and adsorbed on the metals. The CO adsorption tends to be promoted by increasing CO_2 pressure. The type of the adsorbed CO species that significantly increase with the pressure depends on the metals, which is linear CO for Pt, bridge CO for Pd, linear and/or hydride CO for Rh, and linear and bridge CO for Ru. For Pt, the frequency of the linear CO is higher for the HT catalyst having larger metal particles. Similar to Pt, the HT-Rh/Al_2O_3 catalyst shows a higher frequency of the linear and hydride CO species, as compared to the UT catalyst. It is impossible to mention the difference in the frequency of the same type of CO adsorbed

on UT and HT Pd catalysts because the shapes of the CO absorption band at 1760 – 1980 cm^{-1} (bridge CO) are similar between these two samples. For Ru, the shapes of the CO absorption band are different between the UT and HT samples. One can say two possibilities that the sizes of supported Ru particles (2.4 nm, 3.5 nm) influence the relative amounts of linear and bridge CO species or the frequency of the same type of CO adsorption (linear or bridge).

3.3. Formation and Adsorption of CO from CO_2 + H_2 in the Presence of Water (H_2O, D_2O)

In situ FTIR measurements were made for the four UT noble metal catalysts in the presence of water (H_2O) vapor. The spectra obtained in the absence and presence of water at a selected CO_2 pressure of 20 MPa will be compared in the following.

(a) Pt/Al_2O_3 Figure 8A gives FTIR spectra with UT-Pt/Al_2O_3 catalyst after reduction, at a CO_2 pressure of 20 MPa, and after depressurization. The CO adsorption can also be seen after the reduction in the presence of H_2O but most of the adsorbed CO species are bridge type at 1750 – 1850 cm^{-1}.[25-32] The CO_2 pressurization enhances the absorption bands due to the linear and bridged CO at 1900 – 2100 cm^{-1} and 1750 – 1850 cm^{-1}, respectively. Note that the linear CO absorption band seems to lean to lower frequency in the presence of water vapor, which has a vapor pressure of 12.3 kPa at 323 K. Both the linear and the bridge CO species are still adsorbed under ambient conditions after the depressurization.

Figure 8

(b) Pd/Al_2O_3 FTIR spectra with UT-Pd/Al_2O_3 catalyst measured in the presence of H_2O are shown in Figure 8B. No CO adsorption was detected after reduction, similar to the case in the absence of H_2O. An absorption band appeared at 1980 – 1760 cm^{-1} at 20 MP CO_2, which could be assigned to bridge CO species.[33-36] It is noteworthy that the bridge CO absorption band is red-shifted by about 55 cm^{-1} on the addition of water vapor. These bridge CO species remained after the depressurization.

(c) Rh/Al_2O_3 Similar absorption bands were observed with UT-Rh/Al_2O_3 in the presence and absence of H_2O, as shown in Figure 8C. In the presence of water vapor, however, the absorption band of linear and/or hydride CO[37-40] is shifted to a lower frequency range of 2000 – 1880 cm^{-1} while such a significant shift is not seen for the bridge CO absorption at 1880 – 1740 cm^{-1}. After the depressurization, some of those

CO species are still adsorbed in the same shapes of the absorption bands as at 20 MPa CO_2.

(d) Ru/Al_2O_3 Similar effects of water vapor on the formation and adsorption of CO were observed for UT-Ru/Al_2O_3 catalyst (Figure 9). In the presence of H_2O, the CO absorption band seems to lean to lower frequency.

Figure 9

Those results show that the CO absorption band is located at lower frequency in the presence of H_2O, for the linear CO on Pt, for the bridge CO on Pd, for the linear and/or hydride CO on Rh, and for the linear and bridge CO on Ru. Such a red-shift is clearly seen for Pd/Al_2O_3 (Figure 8B) and Rh/Al_2O_3 (Figure 8C) catalysts. The same *in situ* FTIR measurements were made but in the presence of D_2O instead of H_2O. Before these measurements, the absorption of CO dissolved in H_2O and D_2O liquids at 5 MPa was examined by high-pressure ATR-FTIR.[23] The peak positions of ν(CO) absorption band were observed at different frequencies, at 2168 cm^{-1} in H_2O but 2174 cm^{-1} in D_2O. The spectra obtained in the presence of water vapor (H_2O, D_2O) are also given in Figures 8 and 9, in which no difference is seen in the shifts of the CO absorption bands between the spectra collected with D_2O and H_2O. If the adsorbed CO species could interact directly with water molecules in the gas phase and adsorbed on the catalysts, the frequency of the CO absorption bands would be changed on replacing H_2O by D_2O. Then, such a direct interaction should be unlikely in the present systems, which contain only a small amount of water vapor. Furthermore, the FTIR measurements were made with a selected sample of HT-Ru/Al_2O_3 in the presence of H_2O. Figure 9B indicates a symmetrical shape of the CO adsorption band in the presence of H_2O, compared to the band leaning to higher frequency in the absence of H_2O. For this HT sample, an additional absorption band appeared at 1820 – 1730 cm^{-1}, which could be assignable to bridge CO.[41-46]

The adsorption of water may occur on both the Al_2O_3 support and the noble metals. Unfortunately it was difficult to distinguish the water molecules adsorbed on the support and those on the metals by FTIR measurements. This is because the absorption band assignable to the adsorbed water species was very broad due to hydrogen bonding (typical FTIR spectra are given in Supporting Information).

3.4. Adsorption of CO in the Presence of Water (H_2O)

The authors further examined the adsorption of CO (not from CO_2 + H_2) in the presence of water. Figure 10 shows the FTIR results obtained with the four UT-catalysts. The UT-Rh/Al_2O_3 catalyst was previously used for hydrogenation of phenol, in which the catalyst deactivation occurred rapidly in the presence of dense phase CO_2.[15] The catalyst sample was reduced by H_2 and then exposed to CO at atmospheric pressure (Figure 10C). The CO absorption band was seen at the same frequency range of 2060 – 1720 cm^{-1} (line 1, Figure 10), as observed with CO_2 + H_2 (Figure 5), assignable to the linear and/or hydride CO species.[37-40] When the FTIR cell was purged with N_2, the shape of the absorption band changed, in which the absorption at higher frequency became stronger compared to that at low frequency (line 2). Then, H_2O was added and the absorption band at higher frequency was shifted to lower frequency (line 3). This red-shift was also the same as seen in the presence of CO_2, H_2, and H_2O (Figure 8C). After these FTIR measurements, CO was again introduced into the cell but this hardly changed the CO absorption band (line 4). Those results show that the red-shift of CO absorption band at higher frequency occurs when either H_2O co-exists or H_2O is introduced after the adsorption of CO. This is also the case for the other UT-catalysts, as can been seen from Figures 8 and 10.

Figure 10

3.5. Influence of Water Vapor

There was no difference between H_2O and D_2O in the impact on the CO absorption bands. Water molecules in the vapor phase and adsorbed on the catalysts are unlikely to interact directly with the CO species adsorbed on the supported noble metal particles. Considering the above-mentioned FTIR results, we propose for Pt and Pd that water molecules may be more preferentially adsorbed on atomically rough surfaces (high Miller index planes) rather than CO molecules; the CO species may be adsorbed on atomically smoother surfaces (low Miler index planes), as illustrated in Figure 11. Lefferts *et al.* studied the CO adsorption on Pt/Al_2O_3 catalyst in an aqueous phase using ATR-IR technique.[16] They observed a similar red-shift of the CO absorption band and an enhancement of this band in the presence of liquid water. They assume that these effects of water result from direct and indirect interactions of water molecules with the adsorbed CO molecules and with the supported Pt particles. In our experiments, the state of water in our systems is vapor but not bulk liquid; it is unlikely that gaseous water molecules have a significant direct interaction with the adsorbed CO molecules and cause a significant electronic modification of the supported noble metal particles although there is a possibility that some water molecules are adsorbed near the metal

particles. For Ru and Rh catalysts on which linear/hydride CO species and linear/bridge ones are adsorbed, respectively, we propose that the linear CO species are preferentially displaced by water molecules. It is also assumed for Ru and Rh, similar to Pt, that the linear CO species may be adsorbed on atomically rough surfaces while the hydride and bridge ones on atomically smoother surface. Thus, the water molecules are more likely to be adsorbed on rough surfaces than CO and so the water addition prevents the adsorption of CO in the linear type on those metal surfaces. Layman *et al*. studied the CO adsorption on hydrated Ru/Al_2O_3 catalyst using ATR-FTIR and observed a red-shift of the CO absorption band for this sample as compared with untreated one.[19] Considering the dependence of the red-shift on the amount of water adsorbed and on the presence of flowing liquid water, they assumed that this red-shift resulted from dipole-dipole interaction between the co-adsorbed CO and water molecules.

Figure 11

In most of our FTIR experiments, water was already present in the cell when either CO_2 or CO was introduced into it. The authors also made other FTIR experiments in which water was added into the cell after the introduction of CO at ambient pressure (see the above section 3.4.). The same effects of water addition on the CO absorption bands were observed for these two procedures of pre- and post-addition of water. One can say that CO cannot be formed and adsorbed on atomically rough surface sites on which water molecules were pre-adsorbed and that CO species pre-adsorbed on those sites can be replaced by water molecules.

Previously, Thiel and Madey published a comprehensive review on the interaction of water with solid surfaces.[49] It is mentioned that desorption of water adsorbed on rougher (110) surfaces of Pt, Pd, Ni, and Cu occurs at significantly higher temperatures compared to the corresponding smooth (100) and (111) surfaces. The interaction of water of Lewis base character should be stronger with the metal of more Lewis acidic character (more electron-deficient on rougher surfaces), which enhances its ability to accept electrons from the H_2O molecule. This is a simple picture but useful to understand our results. It is speculated that interactions of atomically rough surfaces with water are stronger than those with CO and so the pre-adsorbed CO species on these surfaces may be displaced by the preferential adsorption of water, as observed in our FTIR measurements. It would be useful to compare the heats of adsorption of H_2O and CO on metals. The experimental data with CO[50-52] and a few theoretical studies with H_2O[53,54] can be found in the literature but straightforward comparison of those results

with CO and with H_2O is not significant at present.

A similar effect of the preferential adsorption of foreign species on the CO adsorption was reported in the literature. Previously, Crowell *et al*. studied the adsorption of CO on Rh/Al_2O_3 in which CO was adsorbed in linear, bridge, and twin (dicarbonyl) types.[55] They observed that, when the catalyst was exposed to PH_3, the twin CO was preferentially displaced with the PH_3 species. At 300 K or above, the bridge CO was also displaced by phosphine adsorption. That is, the phosphine is more likely to ligand to these Rh sites and it can replace the CO adsorbed thereon, similar to our system of CO (CO_2 + H_2) and water on Al_2O_3 supported noble metal catalysts.

The present results demonstrate the effects of water vapor on the formation and adsorption of CO in CO_2 + H_2 mixture in the presence of supported noble metal catalysts. In our laboratory, further works are on-going on the same subject in the presence of both water and such an organic substrate as phenol, benzonitrile, and so on by *in situ* FTIR and on the influence of water upon the outcome (total conversion, product selectivity, and catalyst deactivation) of its hydrogenation reaction over supported noble metal catalysts. The work should be interesting for structure-selective catalytic reactions, in which the adsorption of substrate, CO, water, and H_2 on different surfaces of metal particles should be considered.

4. Conclusions

The formation and adsorption of CO from CO_2 and H_2 occur over Al_2O_3-supported Pt, Pd, Rh, and Ru catalysts, proved by *in situ* high-pressure FTIR measurements. The main CO species increasing with CO_2 pressure are linear CO for Pt, bridged CO for Pd, linear and hydride CO for Rh, and linear and bridge CO for Ru. The absorption band of the linear CO species on Pt is red-shifted for the heat-treated catalyst and so these are assumed to indicate lower frequencies on atomically smoother surfaces. When water is present, the CO is also formed and adsorbed on those catalysts but the CO absorption bands appear at lower frequencies. Direct interactions of the adsorbed CO species with water molecules in the gas phase and adsorbed on the catalysts are unlikely to occur but water molecules may be more preferentially adsorbed on atomically rough surfaces rather than the CO molecules.

Acknowledgements

This work was supported by Japan Society for the Promotion of Science with Grant-in-Aid for Scientific Research (B) 22360327 and by the Ministry of Education, Culture, Sports, Science and Technology, Japan, with the Global COE Program (Project No. B01: Catalysis as the Basis for Innovation in Materials Science). The authors are thankful to K. Ohkubo, Faculty of Engineering, Hokkaido University, for his help in TEM measurements.

References

1. A. Baiker, *Chem. Rev.*, 1999, **99**, 453.
2. P. G. Jessop, T. Ikariya, R. Noyori, *Chem. Rev.*, 1999, **99**, 475.
3. P. G. Jessop, *J. Supercrit. Fluids*, 2006, **38**, 211.
4. J. P. Hallett, C. L. Kitchens, R. Hernandez, C. L. Liotta, C. A. Eckert, C. A. *Acc. Chem. Res.*, 2006, **39**, 531.
5. P. G. Jessop, B. Subramaniam, *Chem. Rev.*, 2007, **107**, 2666.
6. A. Kruse, H. Vogel, *Chem. Eng. Technol*., 2008, **31**, 23.
7. G. R. Akien, M. Poliakoff, *Green Chem.*, 2009, **11**, 1083.
8. M. Arai, S. Fujita, M. Shirai, *J. Supercrit. Fluids*, 2009, **47**, 351.
9. D. Ferri, T. Bürgi, A. Baiker, *Phys. Chem. Chem. Phys*., 2002, **4**, 2667.
10. B. Minder, T. Mallat, K. H. Pickel, K. Steiner, A. Baiker, *Catal. Lett*., 1995, **34**, 1.
11. S. Ichikawa, M. Tada, Y. Iwasawa, T. Ikariya, *Chem. Commun*., 2005, 924.
12. M. Burgener, D. Ferri, J.-D. Grunwaldt, T. Mallat, A. Baiker, *J. Phys. Chem. B*, 2005, **109**, 16794.
13. V. Arunajatesan, B. Subramaniam, K. W. Hutchenson, F. E. Herkes, *Chem. Eng. Sci.*, 2007, **62**, 5062.
14. C. D. Zeinalipour-Yazdi, A. L. Cooksy, A. M. Efstathiou, *J. Phys. Chem. C*, 2007, **111**, 13872.
15. S. Fujita, T. Yamada, T. Akiyama, H. Cheng, F. Zhao, M. Arai, *J. Supercrit. Fluids*, 2010, **54**, 190.
16. S. D. Ebbesen, B. L. Mojet, L. Lefferts, *Phys. Chem. Chem. Phys*., 2009, **11**, 641.
17. S. D. Ebbesen, B. L. Mojet, L. Lefferts, *J. Catal*., 2007, **246**, 66.
18. M. Nakamura, M. Ito, *Surf. Sci*., 2001, **490**, 301.
19. A. S. Baird, K. M. Kross, D. Gottschalk, E. A. Hinson, N. Wood, K. A. Layman, *J. Phys. Chem. C*, 2007, **111**, 14207.

20. F. Solymosi, J. Rasko, *J. Catal*., 1989, **115**, 107.
21. X. Meng, H. Cheng, S. Fujita, Y. Yu, F. Zhao, M. Arai, *Green Chem*., 2011, **13**, 570.
22. Y. Akiyama, S. Fujita, H. Senboku, C. M. Rayner, S. A. Brough, M. Arai, *J. Supercrit. Fluids*, 2008, **46**, 197.
23. H. Yoshida, K. Kato, J. Wang, X. Meng, S. Narisawa, S. Fujita, Z. Wu, F. Zhao, M. Arai, *J. Phys. Chem. C*, 2011, **115**, 2257.
24. D. R. Lide, (Ed.), "Handbook of Chemistry and Physics", 79th Edition, CRC, New York, p. 6-3, 1998.
25. C. W. Olsen, R. I. Masel, *Surf. Sci*., 1988, **201**, 444.
26. R. K. Brandt, M. R. Hughes, L. P. Bourget, K. Truszkowska, R. G. Greenler, *Surf. Sci*., 1993, **286**, 15.
27. J. Xu, J. T. Yates, Jr., *Surf. Sci*., 1995, **327**, 193.
28. J. Ruiz-Martínez, F. Rodríguez-Reinoso, *Phys. Chem. Chem. Phys.*, 2009, **11**, 917.
29. R. G. Greenler, K. D. Burch, K. Krezschmar, R. Klauser, A. M. Bradshow, B. E. Hyden, *Surf. Sci*., 1985, **152/153**, 338.
30. M. J. Kappers, J. H. van der Maas, *Catal. Lett*., 1991, **10**, 365.
31. F. Boccuzi, A. Chiorino, E. Guglielminotti, *Surf. Sci.*, 1996, **368**, 264.
32. J. Rasko, *J. Catal*., 2003, **217**, 478.
33. A. M. Bradshaw, F. M. Hoffmann, *Surf. Sci*., 1978, **72**, 513.
34. A. Palazov, G. Kadinov, Ch. Bonev, D. Shopov, *J. Catal.*, 1982, **74**, 44.
35. A. Erdöhelyi, M. Pásztor, F. Solymosi, *J. Catal*., 1986, **98**, 166.
36. A. Wille, P. Nickut, K. Al-Shamery, *J. Mol. Struct.*, 2004, **695-696**, 345.
37. F. Solymosi, A. Erdöhelyi, M. Kocsis, *J. Catal*., 1980, **65**, 428.
38. M. A. Henderson, S. D. Worley, *Surf. Sci*., 1985, **149**, L1.
39. R. W. Matthews, *J. Catal*., 1986, **100**, 275.
40. F. Solymosi, M. Pásztor, *J. Catal.*, 1987, **104**, 312.
41. C. R. Guerra, J. H. Schulman, *Surf. Sci*., 1967, **7**, 229.
42. H. Yamasaki, Y. Kobori, S. Naito, T. Onishi, K. Tamaru, *J. Chem. Soc. Faraday Trans*., 1981, **77**, 2913.
43. C. S. Kellner, A. T. Bell, *J. Catal*., 1981, **71**, 296.
44. F. Solymosi, J. Raskó, *J. Catal*., 1989, **115**, 107.
45. T. Zubkov, G. A. Morgan Jr., O. Kühlert, M. Lisowski, R. Schillinger, D. Fick, H. J. Jänsch, *Surf. Sci*., 2003, **526**, 57.
46. A. S. Baird, K. M. Kross, D. Gottschalk, E. A. Hinson, N. Wood, K. A. Layman, *J. Phys. Chem. C*, 2007, **111**, 14207.
47. F. Solymosi, A. Erdohelyi, M. Lancz, *J. Catal*., 1985, **95**, 567.
48. M. A. Vannice, S. Y. Wang, *J. Phys. Chem*., 1981, **85**, 2543.

49. P. A. Thiel, T. E. Madey, *Surf. Sci. Rep*., 1987, **7**, 211.
50. Somorjai, G. A. "Introduction to Surface Chemistry and Catalysis", Wiley, New York, p.310, 1994.
51. C. Lamberti, A. Zecchina, E. Groppo, S. Bordiga, *Chem. Soc. Rev*., 2010, **39**, 4951.
52. D. Bianchi, *Curr. Top. Catal.*, 2002, **3**, 161.
53. D. D. Bode, Jr., *Adv. Chem. Phys.*, 1971, **21**, 361.
54. J. Ren, S. Meng, *Phys. Rev. B*, 2008, **77**, 054110.
55. G. Lu, J. E. Darwell, J. E. Crowell, *J. Phys. Chem*., 1990, **94**, 8326.

Figure Captions

Figure 1. TEM pictures of UT- and HT-catalyst samples used.

Figure 2. Metal particle size distribution of UT- and HT-catalyst samples determined from TEM pictures. D is the mean particle diameter.

Figure 3. High-pressure FTIR spectra of CO adsorbed on (A) UT-Pt/Al_2O_3 and on (B) HT-Pt/Al_2O_3 (1) after reduction in the absence of CO_2 and at (2) 4 MPa, (3) 8 MPa, (4) 12 MPa and (5) 16 MPa of CO_2 in the presence of 4 MPa H_2 at 323 K and (6) after depressurization to ambient pressure

Figure 4. FTIR spectra of UT-Pt/Al_2O_3 (1) before reduction and after reduction by either 0.1 MPa H_2 (2) or 4.0 MPa H_2 (3) at 343 K.

Figure 5. High-pressure FTIR spectra of CO adsorbed on (A) UT-Pd/Al_2O_3 and on (B) HT-Pd/Al_2O_3 (1) after reduction in the absence of CO_2 and at (2) 4 MPa, (3) 8 MPa, (4) 12 MPa and (5) 16 MPa CO_2 in the presence of 4 MPa H_2 at 323 K and (6) after depressurization to ambient pressure

Figure 6. High-pressure FTIR spectra of CO adsorbed on (A) UT-Rh/Al_2O_3 and on (B) HT-Rh/Al_2O_3 (1) after reduction in the absence of CO_2 and at (2) 4 MPa, (3) 8 MPa, (4) 12 MPa and (5) 16 MPa CO_2 in the presence of 4 MPa H_2 at 323 K and (6) after depressurization to ambient pressure

Figure 7. High-pressure FTIR spectra of CO adsorbed on (A) UT-Ru/Al_2O_3 and on (B) HT-Ru/Al_2O_3 (1) after reduction in the absence of CO_2 and at (2) 4 MPa, (3) 8 MPa, (4) 12 MPa and (5) 16 MPa CO_2 in the presence of 4 MPa H_2 at 323 K and (6) after depressurization to ambient pressure

Figure 8. High-pressure FTIR spectra of CO adsorbed on (A) UT-Pt/Al_2O_3 , (B) UT-Pd/Al_2O_3 and (C) UT-Rh/Al_2O_3 (1) after reduction, (2) at H_2 4 MPa and CO_2 16 MPa and (3) after depressurization to ambient pressure. Dotted, solid and broken lines indicate the spectra in the presence of D_2O, H_2O and absence of water, respectively.

Figure 9. High-pressure FTIR spectra of CO adsorbed on (A) UT-Ru/Al_2O_3 and (B) HT-Ru/Al_2O_3 (1) after reduction, (2) at H_2 4 MPa and CO_2 16 MPa and (3) after depressurization to ambient pressure. Dotted, solid and broken lines indicate the spectra in the presence of D_2O, H_2O and absence of water, respectively.

Figure 10. FTIR spectra for (A) UT-Pt/Al_2O_3, (B) UT-Pd/Al_2O_3, (C) UT-Rh/Al_2O_3 and (D) UT-Ru/Al_2O_3 catalysts (1) after exposure to atmospheric CO for 10min, (2) after purging with N_2, (3) after addition of H_2O, and (4) introduction of CO again.

Figure 11. Illustration of the influence of water on the adsorption of CO on the surface of supported noble metal particles in the absence and presence of water vapor

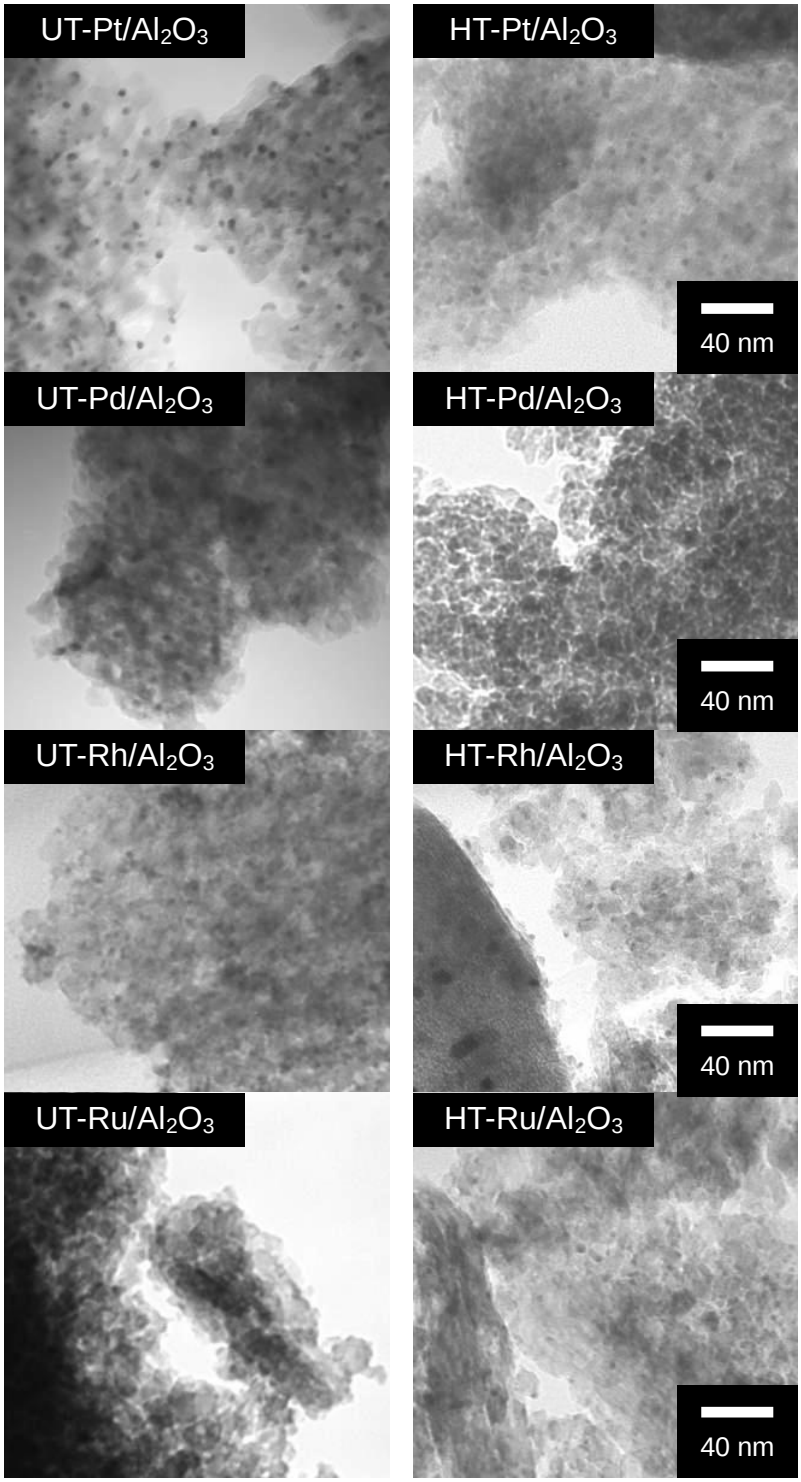


Figure 1. TEM pictures of UT- and HT-catalyst samples used.

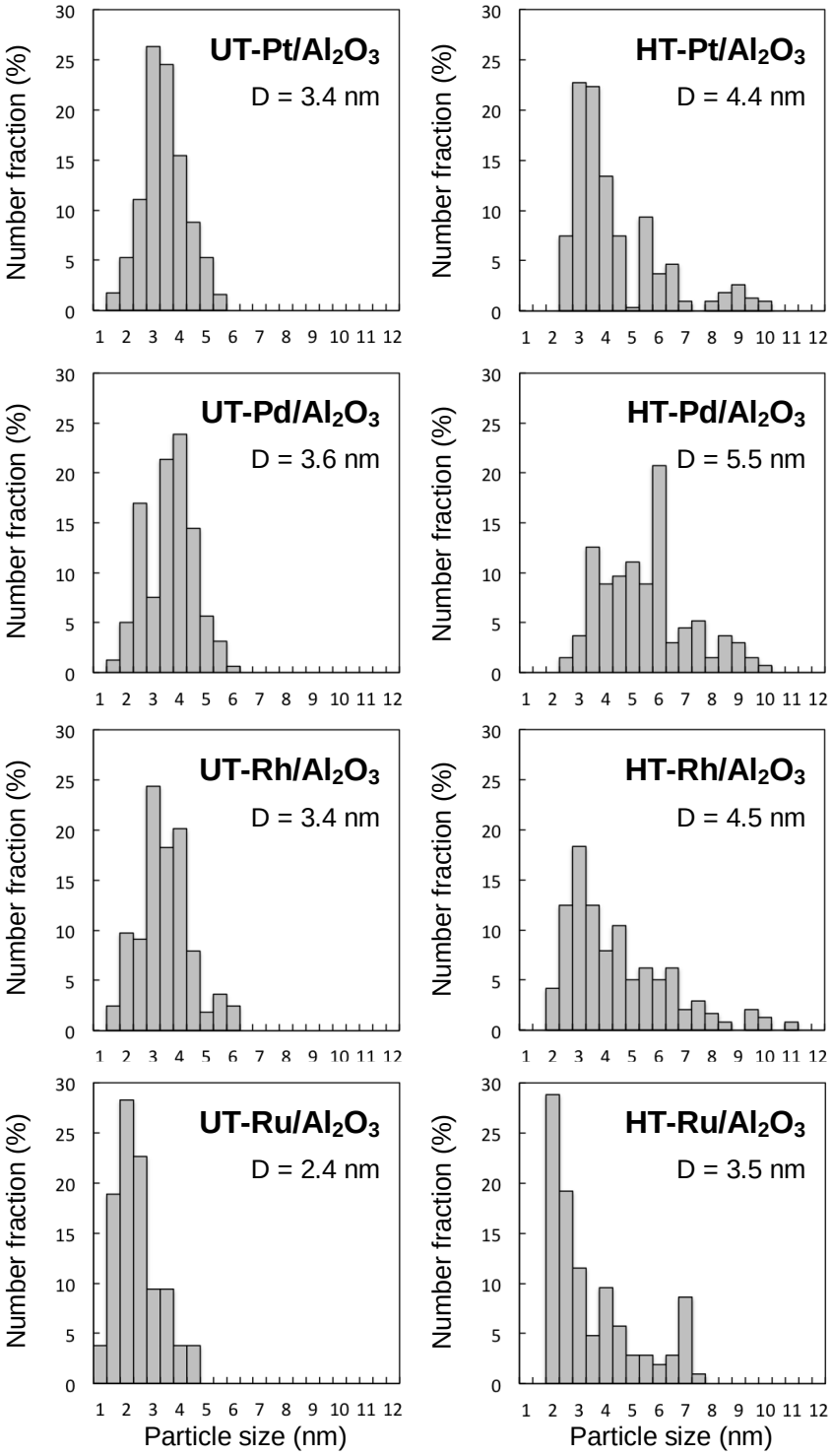


Figure 2. Metal particle size distribution of UT- and HT-catalyst samples determined from TEM pictures. D is the mean particle diameter.

Table 1. Various types of CO adsorption on noble metals according to the literature

Metal	Type of CO adsorbed	Frequency of ν(CO)	Reference
Pt	Linear	2040 – 2095 cm^{-1}	[25-32]
	Bridge	1850 – 1860 cm^{-1}	
Pd	Linear	2050 – 2120 cm^{-1}	[33-36]
	Bridge	1880 – 2000 cm^{-1}	
	Three-fold	1800 – 1880 cm^{-1}	
Rh	Linear	2060 – 2070 cm^{-1}	[37-40]
	Bridge	1855 – 1870 cm^{-1}	
	Twin	2035, 2101 cm^{-1}	
	Hydride	2023, 2033 cm^{-1}	
Ru	Linear	1990 – 2010 cm^{-1}	[41-46]
	Bridge	1870 – 1910 cm^{-1}	

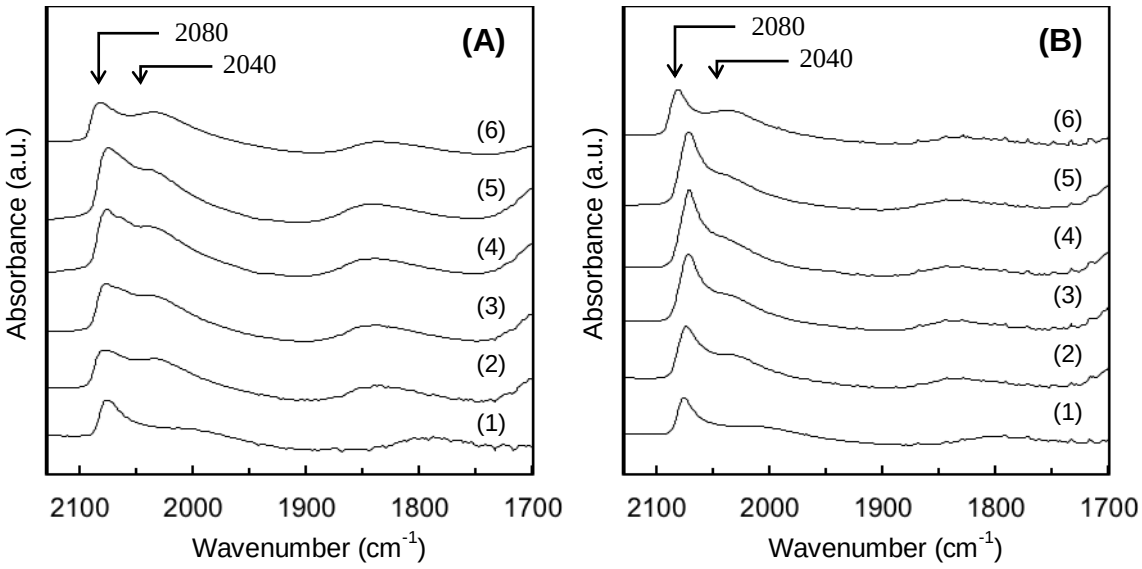


Figure 3. High-pressure FTIR spectra of CO adsorbed on (A) UT-Pt/Al_2O_3 and on (B) HT-Pt/Al_2O_3 (1) after reduction in the absence of CO_2 and at (2) 4 MPa, (3) 8 MPa, (4) 12 MPa and (5) 16 MPa of CO_2 in the presence of 4 MPa H_2 at 323 K and (6) after depressurization to ambient pressure

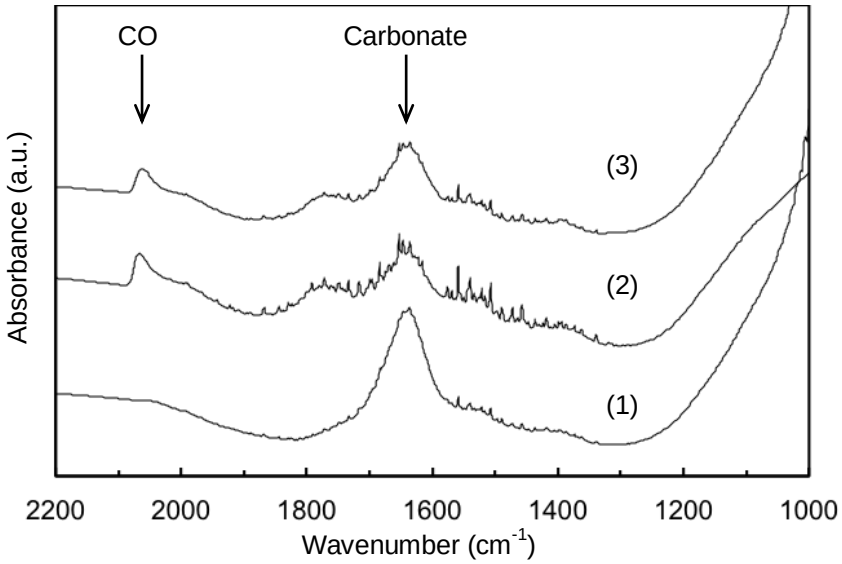


Figure 4. FTIR spectra of UT-Pt/Al_2O_3 (1) before reduction and after reduction by either 0.1 MPa H_2 (2) or 4.0 MPa H_2 (3) at 343 K.

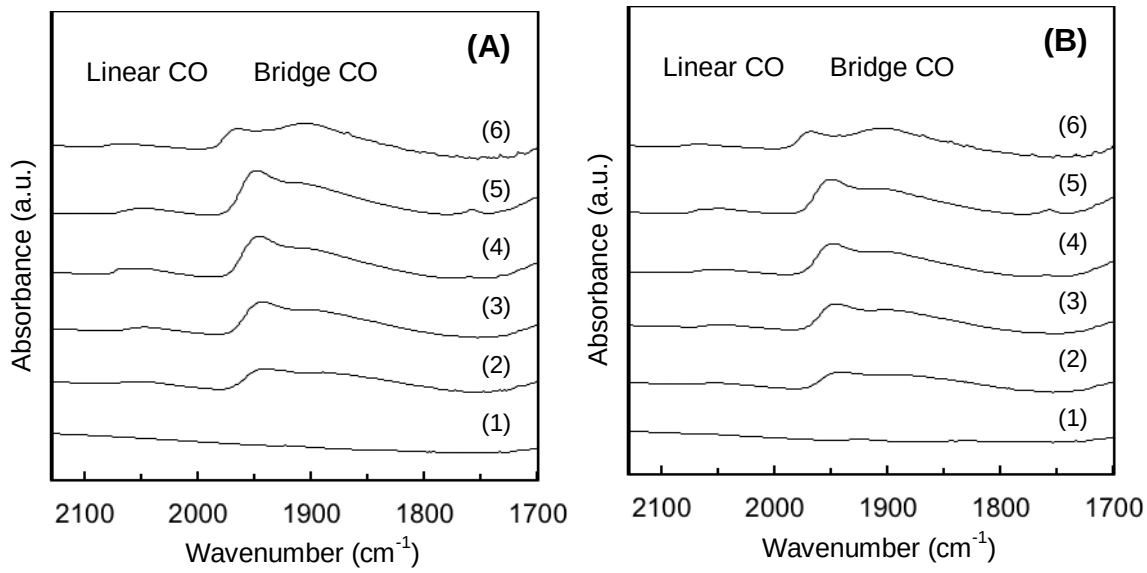


Figure 5. High-pressure FTIR spectra of CO adsorbed on (A) UT-Pd/Al_2O_3 and on (B) HT-Pd/Al_2O_3 (1) after reduction in the absence of CO_2 and at (2) 4 MPa, (3) 8 MPa, (4) 12 MPa and (5) 16 MPa CO_2 in the presence of 4 MPa H_2 at 323 K and (6) after depressurization to ambient pressure

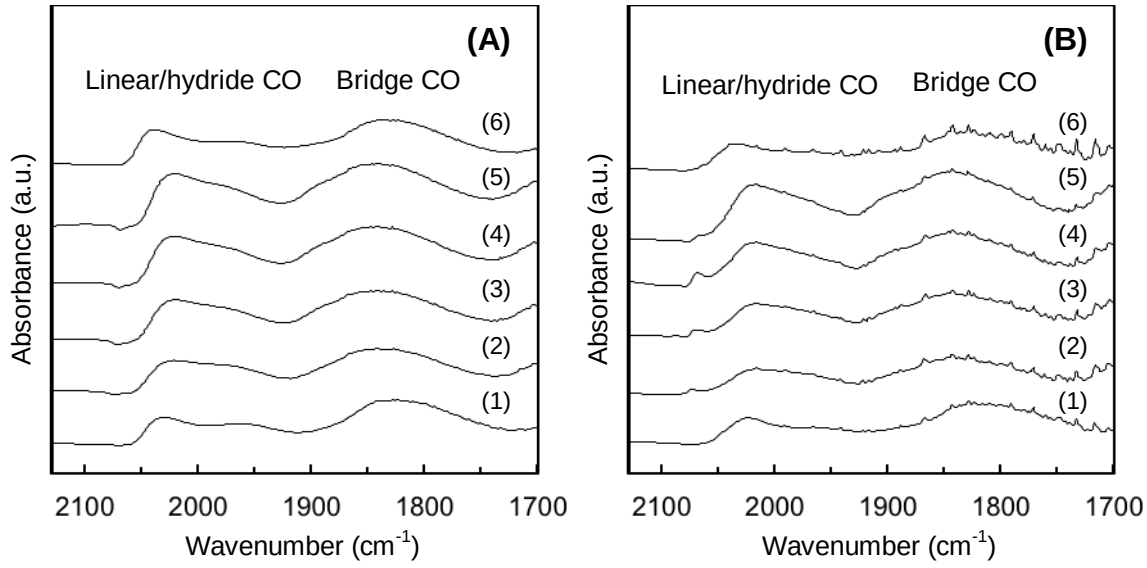


Figure 6. High-pressure FTIR spectra of CO adsorbed on (A) UT-Rh/Al_2O_3 and on (B) HT-Rh/Al_2O_3 (1) after reduction in the absence of CO_2 and at (2) 4 MPa, (3) 8 MPa, (4) 12 MPa and (5) 16 MPa CO_2 in the presence of 4 MPa H_2 at 323 K and (6) after depressurization to ambient pressure

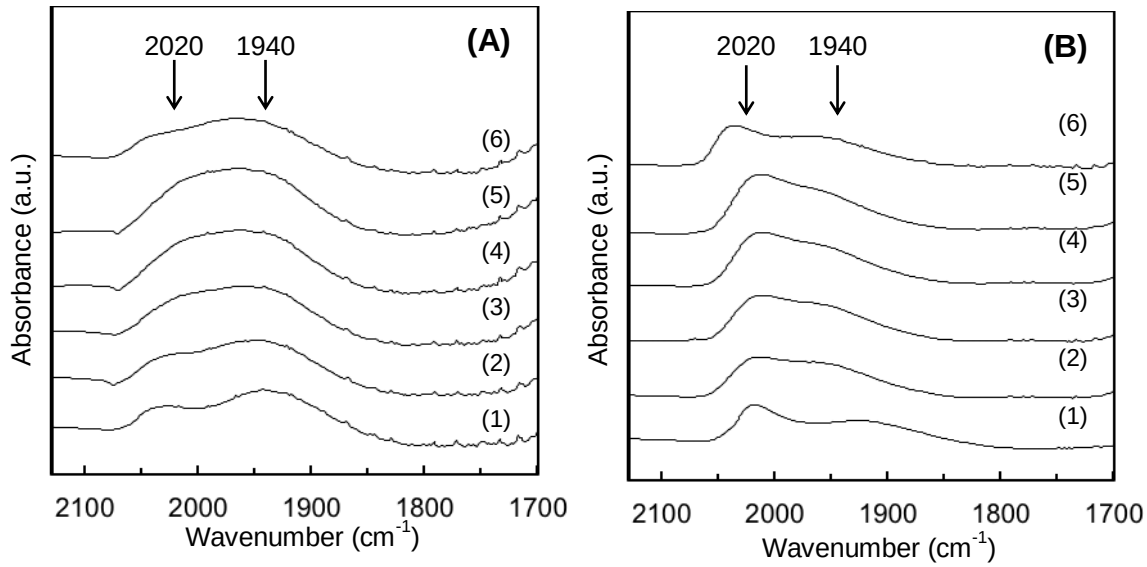


Figure 7. High-pressure FTIR spectra of CO adsorbed on (A) UT-Ru/Al_2O_3 and on (B) HT-Ru/Al_2O_3 (1) after reduction in the absence of CO_2 and at (2) 4 MPa, (3) 8 MPa, (4) 12 MPa and (5) 16 MPa CO_2 in the presence of 4 MPa H_2 at 323 K and (6) after depressurization to ambient pressure

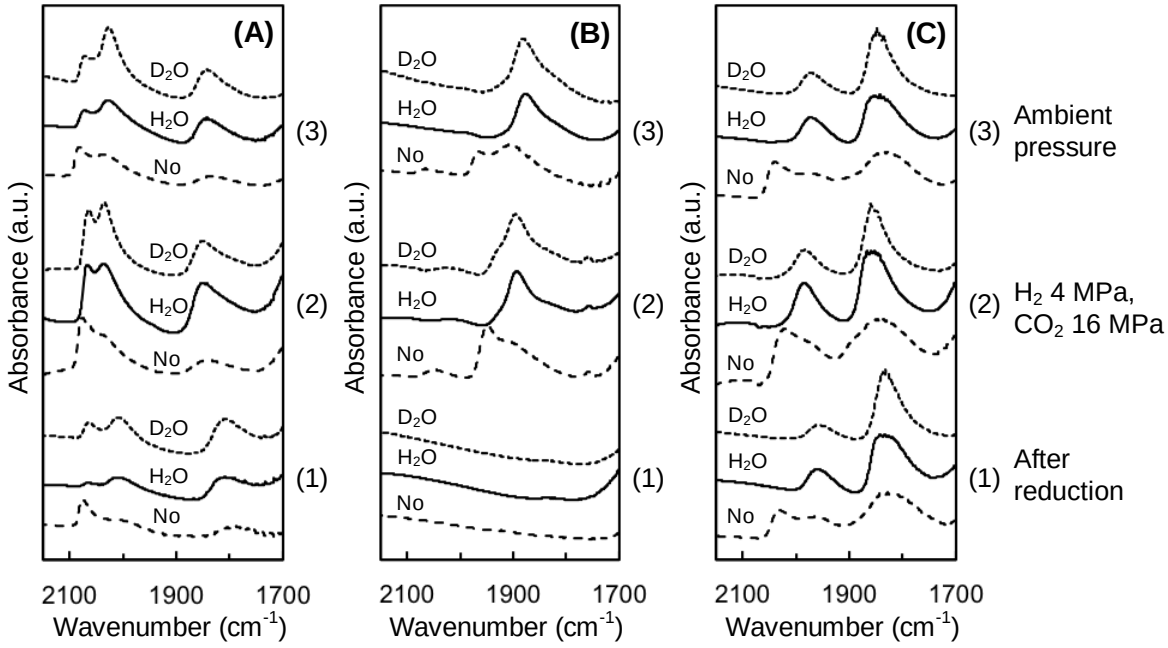


Figure 8. High-pressure FTIR spectra of CO adsorbed on (A) UT-Pt/Al_2O_3 , (B) UT-Pd/Al_2O_3 and (C) UT-Rh/Al_2O_3 (1) after reduction, (2) at H_2 4 MPa and CO_2 16 MPa and (3) after depressurization to ambient pressure. Dotted, solid and broken lines indicate the spectra in the presence of D_2O, H_2O and absence of water, respectively.

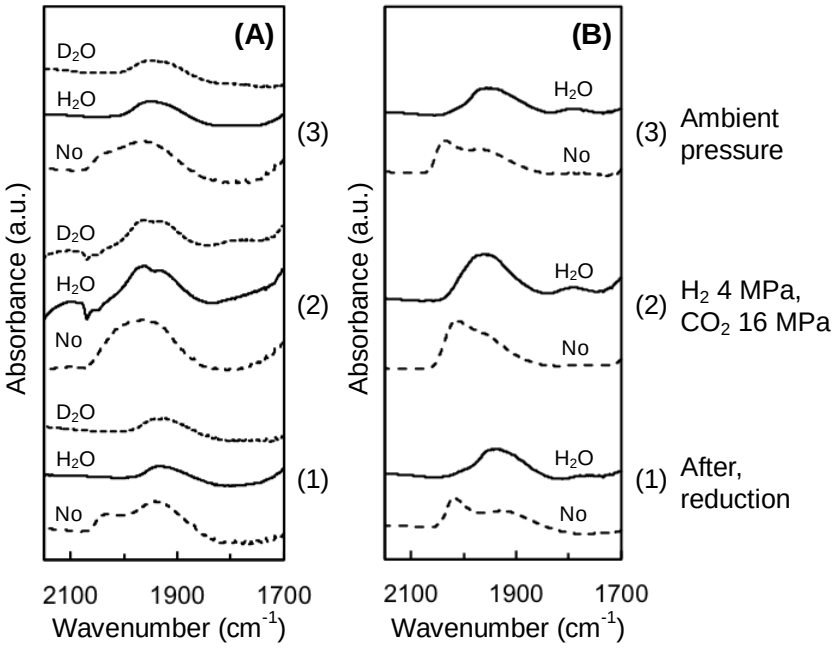


Figure 9. High-pressure FTIR spectra of CO adsorbed on (A) UT-Ru/Al_2O_3 and (B) HT-Ru/Al_2O_3 (1) after reduction, (2) at H_2 4 MPa and CO_2 16 MPa and (3) after depressurization to ambient pressure. Dotted, solid and broken lines indicate the spectra in the presence of D_2O, H_2O and absence of water, respectively.

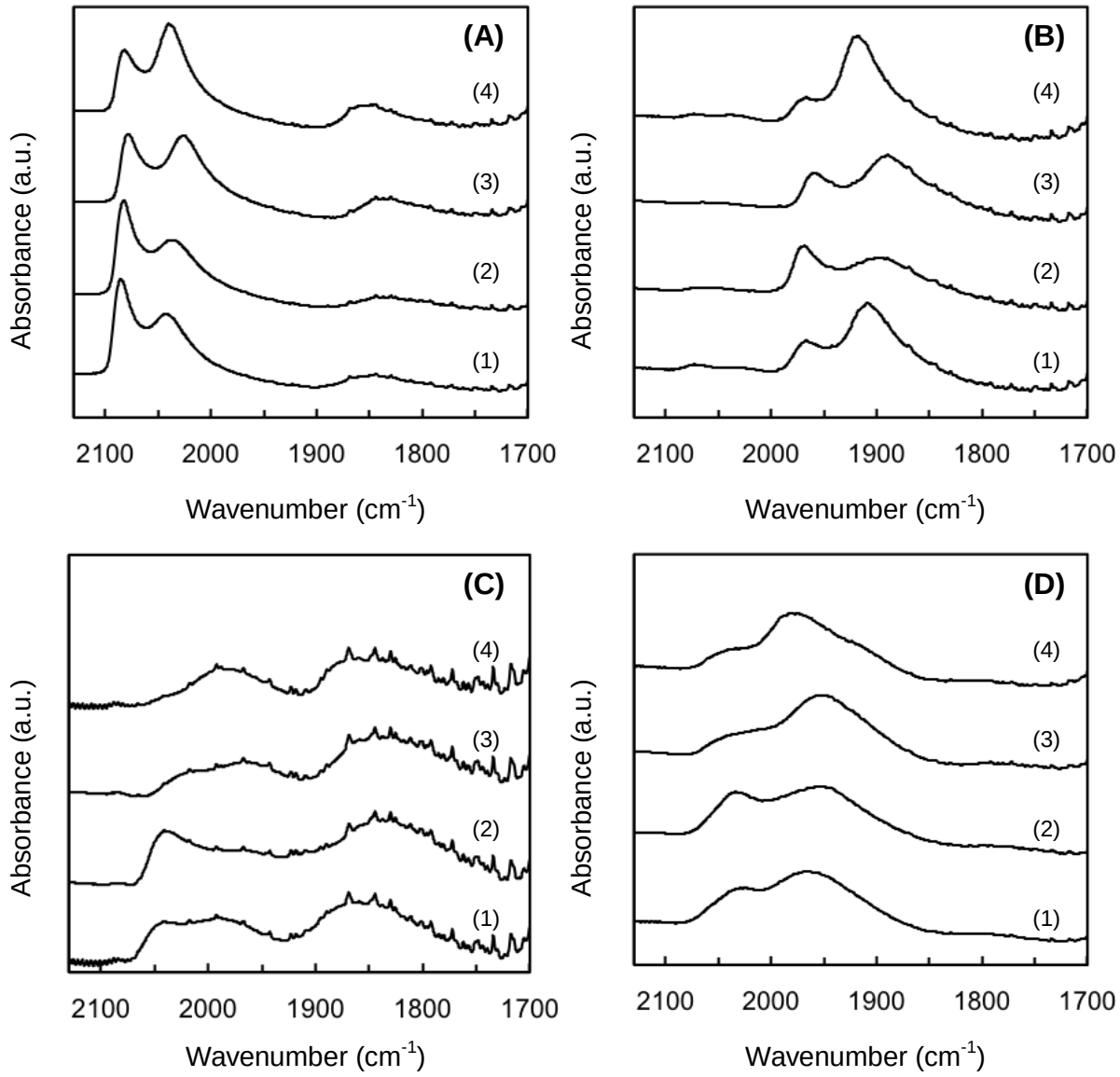


Figure 10. FTIR spectra for (A) UT-Pt/Al_2O_3, (B) UT-Pd/Al_2O_3, (C) UT-Rh/Al_2O_3 and (D) UT-Ru/Al_2O_3 catalysts (1) after exposure to atmospheric CO for 10min, (2) after purging with N_2, (3) after addition of H_2O, and (4) introduction of CO again.

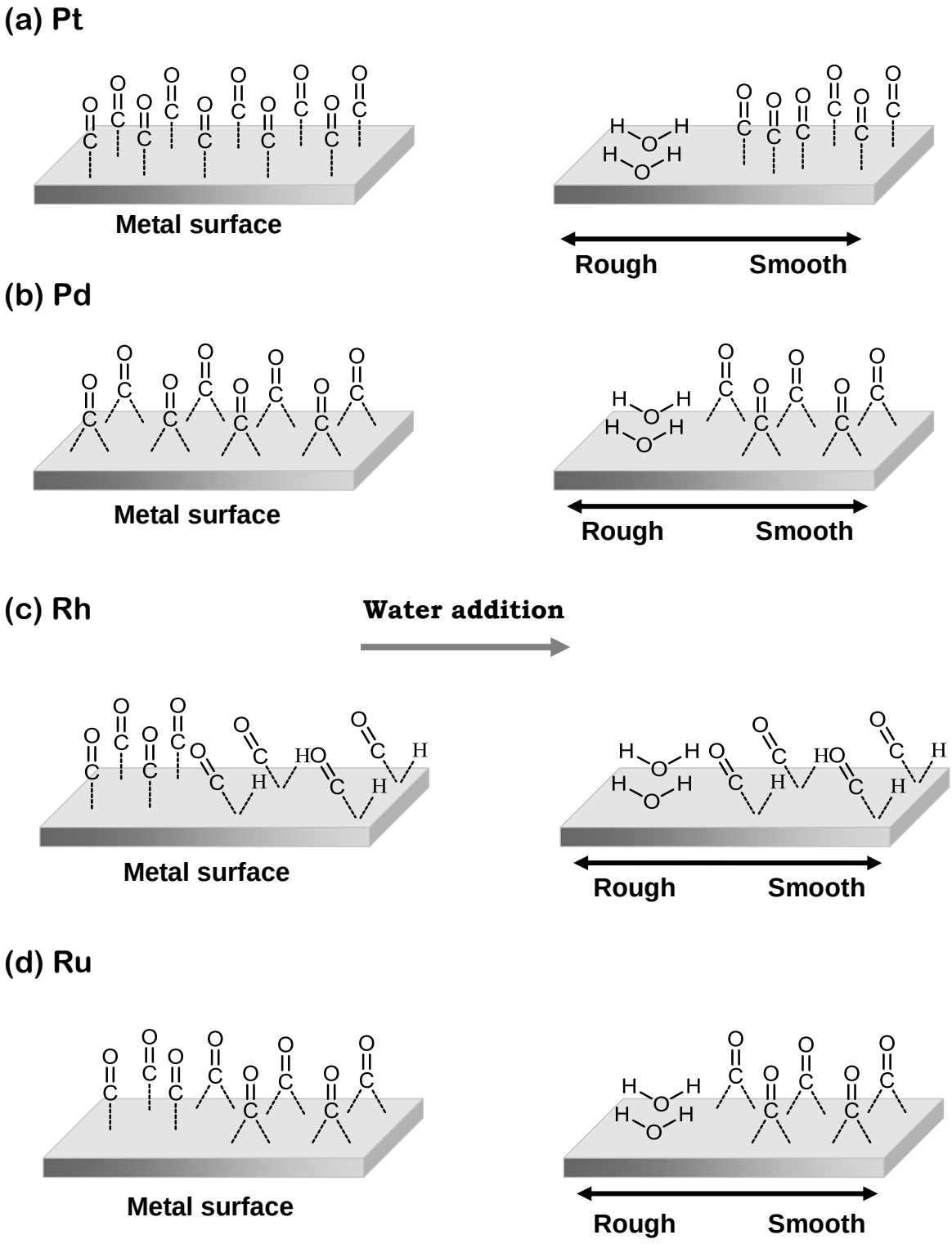
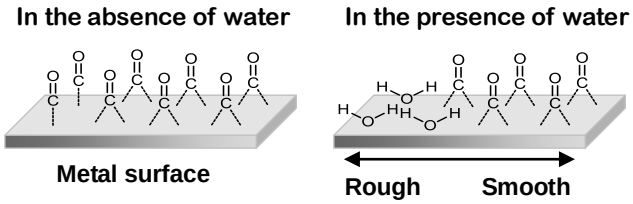


Figure 11. Illustration of the influence of water on the adsorption of CO on the surface of supported noble metal particles in the absence and presence of water vapor

Graphical Abstract

In situ FTIR study on the formation and adsorption of CO on alumina-supported noble metal catalysts from H_2 and CO_2 in the presence of water vapor at high pressures

Hiroshi Yoshida, Satomi Narisawa, Shin-ichiro Fujita, Liu Ruixia, Masahiko Arai



CO formation and adsorption from CO_2 + H_2